

Multi-Wavelength Interferometry for Length Measurements Using Diode Lasers

K. Meiners-Hagen, R. Schödel, F. Pollinger, A. Abou-Zeid

Physikalisch-Technische Bundesanstalt (PTB), Bundesallee 100, D-38116 Braunschweig, Germany, Ahmed.Abu-Zeid@ptb.de

This paper describes the principle of precise length measurements using multi-wavelength interferometry. Three different examples are given in order to demonstrate PTB's ability in this field: 1) Measurements of absolute distances up to 10 m performed by combination of the variable wavelength interferometry with fixed wavelength interferometry using two wavelengths simultaneously, 2) a three-wavelength diode laser interferometer for precision measurements of surface profiles ($< 100 \mu\text{m}$) and 3) PTB's Precision Interferometer for length measurements of prismatic bodies, e.g. gauge blocks, using three wavelengths. The setup and principle of measurements and some results are presented and discussed in each case.

Keywords: interferometry, diode laser, length measurement, long distance, surface profile, gauge blocks

1. INTRODUCTION

THE BASIC principle of length measurement by interferometry is the comparison of a mechanical length (or a distance in space) against a known wavelength of light. Commonly the optical components are arranged such that the light beam double-passes the required length. Therefore, the measurement units are half-wavelengths and the length being measured is expressed as

$$L = \frac{1}{2}\lambda(i + f) \quad (1)$$

where, λ is the wavelength, i is the integer order and f the fractional order of interference. The idea of expressing the length as a multiple of the half-wavelength bases on the observation of interference intensities of two or multiple light waves written as:

$$I = I_0 \left[1 + \gamma \cos\left(\frac{2\pi}{\lambda/2}(z_1 - z_2)\right) \right] \quad (2)$$

in the case of two beam interference. Here, γ is the interference contrast and $z_1 - z_2$ represents the geometrical distance difference between the pathways of the two beams. Thus, a change of one of the path lengths alters the interference intensity periodically in units of $\lambda/2$. The phase difference $\frac{2\pi}{\lambda/2}(z_1 - z_2)$ in (2) may be expressed in terms of

the vacuum wavelength, i.e. by $\frac{2\pi}{\lambda_0/2}n(z_1 - z_2)$. Here, n is the

(air) refractive index within the path and $n(z_1 - z_2)$ represents the differences between the two optical pathways instead of differences between the geometrical distances.

Displacement measurements by a laser interferometer are typically performed by moving one reflector of the interferometer along a guideway and counting the periodic interferometer signal, e.g. the interference fringes. Such a counting technique requires a relatively slow continuous

movement of the reflector along the entire distance to be measured. When the integer order of interference is lost during the movement, only the fractional order of interference is obtained (phase/2π) resulting in a length unambiguity of $\lambda/2$, only. This small unambiguity can be enlarged by using more than one wavelength, i.e. multi-wavelength interferometry.

An ambiguity of lengths measured by single-wavelength interferometry also occurs when there are length discontinuities at the surfaces of objects to be measured resulting in phase steps. Using two wavelengths $\lambda_{1,2}$, the difference of two interferometer phases acts like a single phase of a "synthetic" wavelength $\Lambda = \lambda_1 \cdot \lambda_2 / (\lambda_1 - \lambda_2)$ which is longer than both optical wavelengths. Within half of this synthetic wavelength no counting of interference fringes is necessary. The measurement uncertainty, however, is increased if the measured length L is calculated using the synthetic wavelength. Each uncertainty in both, phase measurements and in the wavelengths is scaled by the ratio of synthetic to optical wavelength. To overcome this problem, it is effective to use the synthetic wavelength only for calculation of the fringe order of the optical wavelengths and benefit from the lower uncertainty of the latter for the length measurement. In this case the measurement uncertainty with the synthetic wavelength must not exceed one quarter of the optical wavelengths to get their correct fringe order. The maximum possible synthetic wavelength is therefore limited. To get a larger range of unambiguity more wavelengths offering different synthetic wavelengths can be used. Starting from the longest one, each synthetic wavelength is used to get the fringe order of the next shorter one and finally that of an optical wavelength.

In general, multiple lasers are necessary for the multi-wavelength technique whose beams have to be aligned on the same path of the interferometer. These must be detected simultaneously after their separation at the interferometer

output for avoiding errors due to the thermal and mechanical drift of the setup.

The effort can be reduced by using wavelength tunable diode lasers. The specific features of such lasers are their tunability by variation of the injection current and the availability of wavelengths from infrared to blue light. This offers a wide range of possible synthetic wavelengths. Depending on the application, the frequency of diode lasers has to be stabilised. By simple parameter stabilisation, i.e. injection current and heat sink temperature, the vacuum wavelength variation is of the order of $\Delta\lambda/\lambda > 10^{-7}$ within days and up to 10^{-5} long term [1]. More sophisticated methods like stabilising the laser on an external cavity or onto atomic or molecular absorption lines, e.g. rubidium, potassium, or iodine, improves the stability by orders of magnitude ($< 10^{-9}$) [2], [3].

This paper gives an overview of three different applications of multi-wavelength interferometry which are well established at PTB: precision measurement of absolute distances (Chap. 2), surface profiles (Chap. 3) and length measurements of prismatic bodies (Chap. 4).

2. PRECISE MEASUREMENTS OF ABSOLUTE DISTANCES

The measurement of distances in the order of ten metres with a relative measurement uncertainty of 10^{-6} is important in a variety of practical applications such as the positioning of components in automotive engineering or aircraft construction, or the inspection of windmill blades. Optical measurements of such distances are typically performed by laser trackers. Recent laser trackers are based on two different length measurement methods: a standard counting interferometer with a HeNe laser and an absolute distance measuring system using a time of flight measurement with an amplitude modulated diode laser. The uncertainty of the absolute length measurement is larger than $10 \mu\text{m}$. Conventional counting interferometers provide a smaller uncertainty but require that the beam follows the reflector movement so that the interference fringes can be counted continuously. In practice, this requires increased efforts and leads to a considerable increase of measurement time. Under well controlled ambient conditions relative measurement uncertainties of 10^{-7} can be achieved.

Absolute distance interferometers (ADI) [4]-[7] achieve a better resolution than systems measuring the time of flight. They could meet the above demand concerning a relative measurement uncertainty of 10^{-6} . Nevertheless, they are not widely used in practice till now, probably due to the complexity of their implementation. Here, an approach to an ADI based on a homodyne interferometer with two diode lasers is presented.

2.1. PRINCIPLES OF MEASUREMENT

2.1.1. THE VARIABLE SYNTHETIC WAVELENGTH APPROACH

Absolute distance interferometry with a variable synthetic wavelength is performed by use of a laser whose emission frequency ν can be tuned continuously. Diode lasers, with a large mode-hop free tuning range for this purpose, are usually used. In the case of an external cavity diode laser the tuning of the laser frequency $\Delta\nu$ (typically $50\dots100 \text{ GHz}$) is obtained by changing the diffraction angle by tilting the grating (Littrow type) or by tilting the mirror (Littman type) in the external resonator. In case of a distributed feedback laser diode (DFB) the injection current is modulated. The laser frequency is usually tuned periodically by an oscillator.

In an interferometer the phase Φ is generally given by

$$\Phi = \frac{4\pi}{\lambda_0} nL = \frac{4\pi\nu}{c} nL \quad (3)$$

Here, λ_0 is the laser wavelength in vacuum, ν the laser frequency, c is the velocity of light in vacuum, L is the arm length difference in the interferometer, and n is the refractive index of air. The latter requires the measurement of the ambient parameters (temperature, air pressure, humidity) and can be derived from an Edlén-type empirical equation [8].

In an absolute interferometer the length L_{ADI} , i.e. the length difference between the two interferometer arms, can be calculated from the phase change $\Delta\Phi$ caused by the frequency tuning $\Delta\nu$ according to

$$L_{ADI} = \frac{c}{4\pi n} \frac{\Delta\Phi}{\Delta\nu} \quad (4)$$

In this case $\Delta\nu$ may be obtained from the transmission of a Fabry-Perot resonator. The laser frequency at the transmission peaks is given by $\nu = \nu_0 + i \cdot FSR$, with FSR being the free spectral range of the resonator, i the number of the transmission peaks which are swept during the tuning, and ν_0 the initial frequency. Thus, the factor $\Delta\Phi/\Delta\nu$ in (4) is obtained as the slope of a linear interpolation of the phases $\Delta\Phi(i)$.

Alternatively, the light of the laser can be coupled simultaneously into the ADI and into a reference interferometer of a known length L_{ref} which has to be determined independently. The length L_{ADI} of the ADI can be calculated from the phase changes in the ADI ($\Delta\Phi_{ADI}$) and in the reference interferometer ($\Delta\Phi_{ref}$):

$$L_{ADI} = L_{ref} \frac{n_{ref}}{n_{ADI}} \frac{\Delta\Phi_{ADI}}{\Delta\Phi_{ref}} \quad (5)$$

The refractive indices have to be considered in the ADI (n_{ADI}) and in the reference interferometer (n_{ref}). If both interferometers are placed closely together, the refractive indices are almost equal, and their influence is almost nullified. During the tuning of the laser frequency several phase values from both interferometers are recorded and then fitted to a linear function which passes the origin. The number

of data pairs for the fit is only limited by the measurement rate (speed of the detector electronics and A/D conversion). This is a significant advantage compared to the use of a Fabry-Perot resonator as reference because in the latter case only a limited number of transmission peaks can be used for data sampling.

Length changes, due to, e.g. reflector vibrations that occur during the tuning of the laser frequency, contribute considerably to the measurement uncertainty of frequency sweeping interferometry. If the length is not constant in time, the measured phase values $\Delta\Phi_{ADI}$ in (4) and (5) correspond to different values of L_{ADI} . Variations of L_{ADI} are scaled up with the ratio $v/\Delta v$, which is typically in the range of 10^3 to 10^4 . In the case of vibrations, the impact on L_{ADI} can be reduced by averaging over an appropriate number of single measurements.

In our approach to absolute distance interferometry, we monitor changes of the length L_{ADI} during tuning by a conventional counting interferometer with a permanently frequency stabilised laser with the vacuum wavelength λ_1 , which runs parallel to the ADI. The phase change $\Delta\Phi_{ADI}$ of the ADI originating from frequency tuning is corrected by the result of the stabilised laser:

$$\Delta\Phi_{ADI}(\text{corr.}) = \Delta\Phi_{ADI} - \frac{\lambda_1 n_2}{\lambda_2 n_1} \Delta\Phi_1 \quad (6)$$

Here, $\Delta\Phi_1$ is the measured phase change of the conventional interferometer. n_1 and n_2 are the refractive indices for λ_1 and λ_2 in the ADI. They differ from each other only due to the dispersion in air since both beams are on the same optical path. The central vacuum wavelength of the tuned laser is denoted as λ_2 . By inserting (6) into (5), the final result L_{ADI} for the coarse measurement is obtained.

2.1.2. THE FIXED SYNTHETIC WAVELENGTH APPROACH

The range of unambiguity can be extended by using more than one wavelength in the interferometer. The output intensity of a two beam interferometer is given in (2). The argument of the cosine function is the phase Φ of the interferometer signal and can be written as in (3). If the interferometer is operated with two optical wavelengths λ_1 and λ_2 the difference $\Delta\Phi_{synth}$ between the phases is given by

$$\begin{aligned} \Delta\Phi_{synth} &= \Phi_2 - \Phi_1 = \left(\frac{4\pi}{\lambda_2} - \frac{4\pi}{\lambda_1} \right) nL = \frac{4\pi}{\Lambda} nL, \\ \Lambda &= \frac{\lambda_1 \lambda_2}{\lambda_2 - \lambda_1} \end{aligned} \quad (7)$$

The phase difference $\Delta\Phi_{synth}$ corresponds to the phase of the fixed synthetic wavelength Λ . It is larger than the optical wavelengths and determines the range of unambiguousness to $\Lambda/2$. Here the wavelengths are assumed to be closely together so that the refractive index n is approximately identical for

both wavelengths. By considering not only the phase difference but the phases itself, the range of unambiguousness can be extended to more than $\Lambda/2$. After moving the reflector by one period of the synthetic wavelength the phase difference $\Delta\Phi_{synth}$ is the same as before, but the single phase values are usually different after the movement. When the phase measurement itself has a low uncertainty, a “phase recovery criterion” can be applied. Basically, such criterion corresponds to the “method of exact fractions” as further discussed in Chap. 4.

If several synthetic wavelengths are used, the longest one determines the unambiguous measuring range. The measurement uncertainty increases according to the ratio of the synthetic to the optical wavelengths. Therefore, the shortest synthetic wavelength gives the lowest uncertainty. The length result from one synthetic wavelength is typically used to determine the fringe order of the next shorter synthetic wavelength.

Since the absolute distance interferometry with a variable synthetic wavelength as described in Chap. 2.1.1 uses a frequency stabilised laser 1 and a second frequency swept laser 2, it seems straightforward to expand this setup for a measurement with a fixed synthetic wavelength. For that purpose the frequency sweep from laser 2 has to be stopped, and the laser has to be stabilised. The measurement consists of two steps: First, the integer order of interference for Λ is determined by the measurement with variable synthetic wavelength according to (5) and (6). After switching the modulated laser in the stabilised mode, the fractional order of interference is determined according to (7). Thus, the final result L of the two-stage length measurement is

$$L = \left\lfloor \frac{L_{ADI}}{\Lambda/2} - \frac{\Delta\Phi_{synth}}{2\pi} + \frac{1}{2} \right\rfloor \frac{\Lambda}{2} + \frac{\Delta\Phi_{synth}}{2\pi} \frac{\Lambda}{2} \quad (8)$$

where $\lfloor x \rfloor$ denotes the floor function which returns the largest integer which holds the condition $\leq x$. The synthetic phase $\Delta\Phi_{synth}$ is measured without counting fringes and is in the range $\Delta\Phi_{synth} \in [0 \dots 2\pi]$. The subtraction of the term with $\Delta\Phi_{synth}$ and the addition of $\frac{1}{2}$ in the floor function have a practical reason: without these terms the equation is mathematically correct, but the measurement uncertainties lead to a scatter of L_{ADI} . At the border between two fringe orders even a small scatter can lead to the wrong fringe order. Both terms shift the value in the floor function mathematically to constant levels of $1/2, 3/2, 5/2, \dots$, which lead to the fringe order $0, 1, 2, \dots$. Therefore, scatter smaller than $\Lambda/4$ has no influence on determining the fringe order. It should be noted that this absolute interferometer can also be applied as laser tracker, i.e. as a standard counting interferometer using the permanently stabilised laser.

2.2. EXPERIMENTAL SETUP AND RESULTS

The optical setup of our ADI as a homodyne Michelson interferometer is depicted in Fig.1. Laser 1 is a Littrow type extended cavity diode laser (ECDL) operating at approx. 770.1 nm wavelength, and laser 2 is a Littman type ECDL at approx. 766.7 nm wavelength. Both lasers are equipped with antireflection coated laser diodes. For both ECDLs, a small amount of their intensity is split off by a combination of a half-wave plate and a polarizing beam splitter and is fed to a setup using polarization-optical differential detection for the stabilisation to Doppler-reduced potassium (K) absorption lines as described for Rubidium in [2]. Laser 1 is permanently stabilised to a K-D1 line. The emission frequency of the laser 2 is tuned by the use of a programmable function generator. A low pass filtered and smoothed triangle signal with a frequency of 5...10 Hz is used for the modulation.

A portion of the modulated laser's intensity is coupled into the reference interferometer which is placed in a temperature stabilised box. For the ADI, both laser beams are coupled into one polarisation maintaining single mode fibre in order to ensure that they traverse the interferometer on identical paths. By the use of a half-wave plate in front of and a polarizer behind the fibre, matching of the polarization of the laser's light with the fibre axis is achieved. At the interferometer output the two beams are separated by a grating for detection. The interferometer is composed of a polarizing beam splitter and two triple reflectors.

The interference signals are processed within the detectors in such a manner that two signals are obtained which are shifted by 90° to each other. To obtain these quadrature signals for the modulated laser, it has turned out advantageous to use Fresnel rhombi instead of quarter wave plates since the retardation for the latter is more strongly dependent on the wavelength. The quadrature signals for the ADI, the reference interferometer, and the counting interferometer operated by laser 1 are recorded with an acquisition rate of 250000 samples s^{-1} by a 16-bit, 8 channel A/D converter card. First, a data block is sampled with a length depending on the averaging time. The raw sine-cosine values are processed by a Heydemann correction [9]. Since the frequency modulated laser has a slight amplitude modulation, the sine-cosine signals do not follow an ellipse but have a slightly spiral shape. The amplitude modulation is $\approx 5\%$ of the total intensity so that for a few 2π periods an ellipse is a good approximation. Therefore, several ellipse fits over a few periods instead of one over all data points are calculated.

Subsequently, single phase values are calculated by the arctan function, and are sorted according to the rising and falling edges of the modulation. The phase of the ADI is corrected by the phase of the stabilised laser interferometer according to (6). For each edge, the phases of the ADI and the reference interferometer are linearly interpolated by a least

square fit with the axis intercept set to zero. With the slope, the length L_{ADI} is determined according to (5).

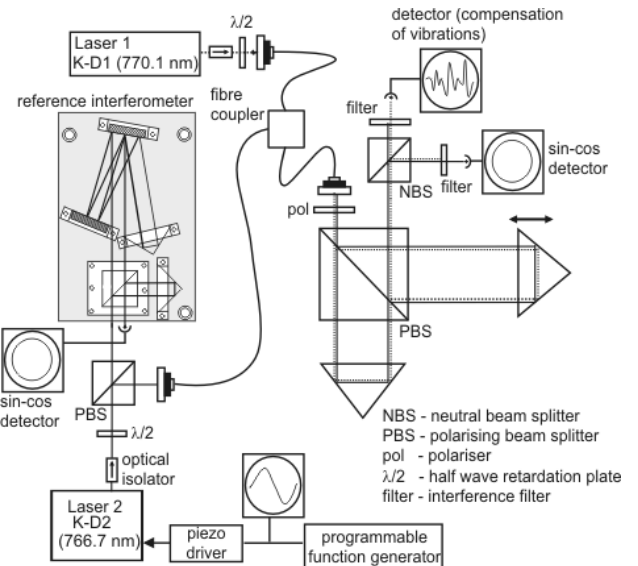


Fig.1 Optical setup of the absolute distance interferometer with two ECDLs. The light of both diode lasers is coupled into a Michelson interferometer via one polarization maintaining single mode fibre. For clarity, the details for the stabilisation of the ECDLs to potassium absorption lines are not shown

For the fixed synthetic wavelength approach, laser 2 is stabilised on a K-D2 absorption line at approx. 776.1 nm giving a synthetic wavelength of $\approx 173 \mu m$. The fractional part of the length can be directly evaluated from (8) after the Heydemann correction. In the case of stabilised lasers, it is sufficient to determine the parameters for the Heydemann correction during a slow movement of the measurement reflector prior to the measurement.

Length measurements with the setup shown in Fig.1 were performed at the geodetic base of the PTB. It consists of a 50 m long bench with a moving carriage and is equipped with a conventional counting HeNe laser interferometer with a folded beam path, which was used as reference. The refractive index of air is determined by the Edlén equation [8]. The environmental parameters were measured by one air pressure and one relative humidity sensor, and temperature by PT100 sensors placed at an interval of 2.5 m along the bench. Results of measurements for lengths of ~ 2 m were published in [7]. In the following results for approx. 10 m distance are discussed.

Fig.2 shows the stability of the ADI at a length of approx. 10.15 m for three different averaging times. The standard deviations of the length values from Fig.2 are plotted in Fig.3 versus the averaging time. The single edges of the 6 Hz modulation signal show a standard deviation of $51 \mu m$ and decrease almost according to $1/\sqrt{N}$ with the number of

samples N averaged. For suitable averaging times of 1 s...2 s the standard deviation is below 15 μm . The interpolation of the length with the synthetic wavelength for the K-D1 and K-D2 stabilised lasers ($\approx 173 \mu\text{m}$) requires an uncertainty smaller than $\Delta/4 \approx 43 \mu\text{m}$.

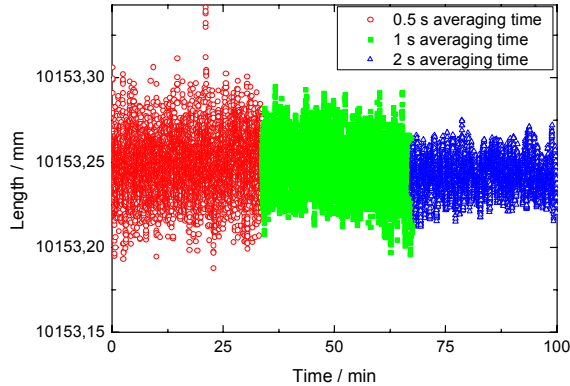


Fig.2 Stability of the ADI for different averaging times at a length of approx. 10 m.

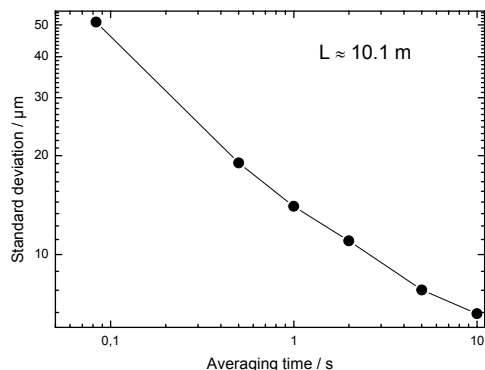


Fig.3 Standard deviation of the ADI for different averaging times from the data of Fig.2. The shortest time of approx. 83 ms corresponds to one edge of the 6 Hz modulation signal.

A comparison of the ADI to the counting HeNe laser interferometer is shown in Fig.4 with an averaging time of 2 s. Except for two points, the difference for all data points is below 43 μm . Therefore, the resulting synthetic wavelength from the stabilisation on potassium absorption lines is sufficient. With a longer averaging time longer measuring lengths for the ADI should be possible.

The combined evaluation of ADI and fixed synthetic wavelength measurements as described in Chap. 2.1 leads to results like the one presented in Fig.5.

According to Fig.5, the deviation between the ADI and the HeNe interferometer is below $0.5 \mu\text{m} + 0.5 \mu\text{m}/\text{m}$ except of three points. Thus, the well known approach of an absolute interferometer with one laser with modulated laser frequency

and a second, frequency stabilised laser for compensation of vibrations can be improved by frequency stabilising both lasers and using the synthetic wavelength for further interpolation of the result.

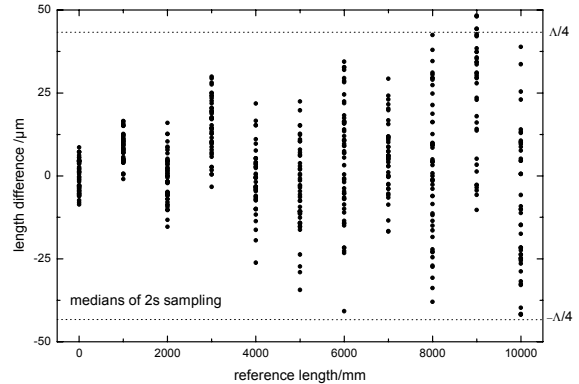


Fig.4 Difference between the ADI with an averaging time of 2 s and a counting HeNe laser interferometer.

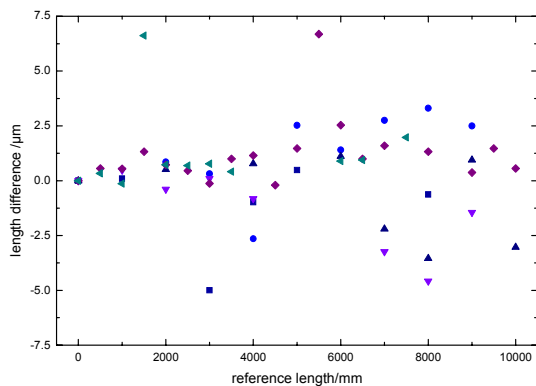


Fig.5 Difference between the absolute interferometer and a counting HeNe laser interferometer as a function of the reference length after evaluation according to eq. (8). The different symbols denote individual measurements.

3. PRECISE LENGTH MEASUREMENTS OF SURFACE PROFILES

High precision measurements of surface topography and properties like roughness are important tasks in quality assurance and control. There are a number of different technologies which differ by the measurement principle, operating complexity, resolution, and measuring range. Interferometric methods have a very high resolution within the nanometre range. Laser interferometers, however, are giving ambiguous results for distance variation of more than half the wavelength λ , e.g. due to steps in the surface. Nevertheless, using the multi-wavelength technique the interferometric measurement of surface profiles is possible.

For the measurement of surface profiles the measuring range of the interferometer was supposed to be in the order of 100 μm . Using parameter stabilised laser diodes three wavelengths were necessary. Wavelengths of 789.5 nm,

822.95 nm, and 825.3 nm were chosen which lead to synthetic wavelengths of approx. 14.0 μm , 14.8 μm , and 289 μm .

A modulation technique allows the separation of the wavelengths at the interferometer output. The injection current of the three laser diodes is modulated with different frequencies ω_m around 1 MHz. This results in a modulation of the laser frequency by Δv and a modulation of the interferometer phase. At the interferometer output a spectrum appears with harmonics of ω_m . The amplitude of two adjacent harmonics is proportional to the sine and cosine of the interferometer phase. Lock-in amplifiers detecting at the second and third harmonic give a quadrature signal [10].

The different modulation frequencies of the laser diodes allow the simultaneous detection of the three interferometer signals with only one photo detector. The optical setup, sketched in Fig.6, is also simplified by the modulation technique.

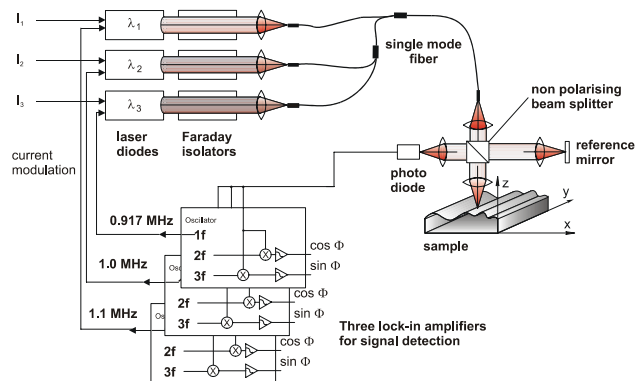


Fig.6 Optical setup of the surface profilometer with a multiple wavelength diode laser interferometer

The beams of the diode laser are coupled into one single mode fibre. Faraday isolators protect the diodes from feedback light. The fibre is connected to a simple unbalanced Michelson interferometer without polarization optical components. One arm of the interferometer leads to the reference mirror, the light of the other arm is focused onto the sample. Depending on the measurement range in z-direction, i.e. focus depth, and on the lateral resolution, the focal length of the objective lens can be chosen suitable for surfaces under investigation. The sample can be moved in both lateral directions with mechanical translation stages by approximately 15 cm.

The developed diode laser profilometer was tested using a PTB depth setting standard chosen as a test surface with a well-known surface topography [11]. This standard is a glass block, 8 mm thick, 20 mm wide, and 40 mm long with six grooves of circular profile, the depth ranging from 190 nm to 9.2 μm . The reference values of this standard have been reproduced within the uncertainties stated for the depth setting standard as shown in Table 1.

Table 1 Comparison of the measured groove depths with the reference values of depth setting standard

Diode laser profilometer / nm	PTB reference value / nm
196	191 \pm 6
445	440 \pm 6
945	952 \pm 10
2130	2141 \pm 32
4520	4543 \pm 48
9225	9208 \pm 80

All scans on flat surfaces, like mirror substrates, exhibit periodic structures with height variations of up to 250 nm. These structures can be clearly assigned to unwanted vertical movement of the x-y translation stages. To get more information about this error source a second translation stage with a piezo actuator (PZT) was mounted on top of the mechanical stage. Two scans were performed with the depth setting standard placed on the PZT stage, one with the PZT turned off and the other with a displacement of 47 μm from the PZT. A part of the scan near the groove with \approx 190 nm depth is shown in Fig.7. The coordinate is related to the surface of the depth setting standard so that the groove is located at the same position in both scans. A wavy structure with up to 25 nm amplitude and a sharp decrease in height at $x \approx 1$ mm is shifted by 47 μm between the scans. These effects are caused by a vertical movement of the translation stage.

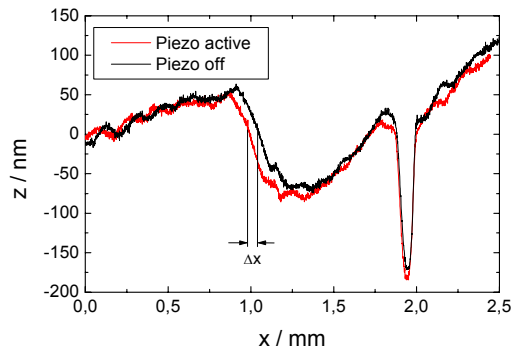


Fig.7 Groove of a depth setting standard, scanned without and with displacement from the piezo stage of 47 μm .

These errors have only little influence for measuring the groove depths. The depths were determined as the difference between the deepest point in the groove and the surface around. Within the maximum width of the grooves of 0.3 mm the deviations from the translation stages can be linearised in most cases and they only appear as an additional tilt of the surface. The translation stage therefore leads to an additional uncertainty of the order of 25 nm, corresponding to the wavy structures in Fig.7. If the scan lines are longer than the period

of the stage of approx. 4 mm, the stage error fully enters the result. With an additional piezo driven x-y stage it is in principle possible to correct the errors of the mechanical translation stages by measuring with different displacements. The measurement uncertainty of the profilometer is therefore limited by the quality of the translation stages.

The uncertainty of the interferometer itself is estimated to approximately 20 nm for a 100 μm measuring range and an arm length difference of 10 cm [10]. Uncertainty contributions arise from the long and short term wavelength stability of diode lasers used (1 nm and 10 nm, respectively). Contributions due to changes of the refractive index of air are negligible. A further uncertainty contribution can arise from the phase measuring, e.g. due to the lock-in amplifiers, or optical quality of the surface. This contribution amounts to approx. 4 nm for smooth, highly reflective surfaces.

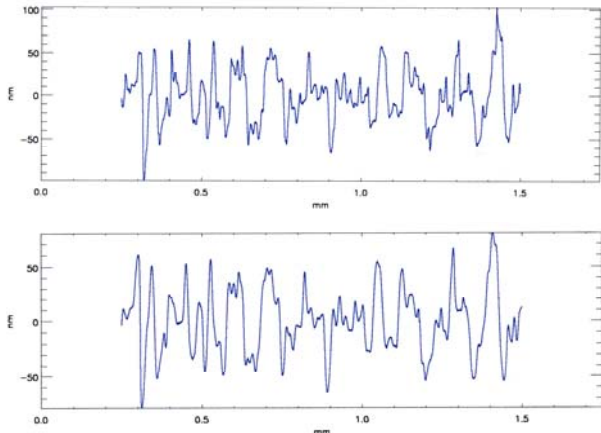


Fig.8 Surface profile measured with a contact stylus instrument (upper curve) and with the interferometer (lower curve)

On rough surfaces the interference contrast varies over the sample which affects the interferometer signal. Three so-called "superfine roughness standards" with R_z values between 134 nm and 450 nm were measured to investigate the limits of the interferometer on rough surfaces. These standards are cylindrical disks with approx. 50 mm diameter with a 4 mm wide rough zone around the centre. Fig.8 shows a part of the surface profile of a roughness standard with an average maximum height $R_z = 134$ nm as measured with the diode laser interferometer in comparison with the contact stylus instrument. Apparently the profile is well reproduced by the interferometer. However, fine details like the sharp spike near position 1.4 mm and the narrow groove near 0.3 mm are smoothed by the interferometer. This is caused by the focus diameter of approx. 2 μm of the microscope objective used for these measurements so that the measured height values are averaged over this range. This smoothing leads to an apparent decrease of the roughness. All roughness parameters derived

from the interferometer data are smaller than their reference values from the calibration with a contact stylus instrument. The roughness average R_a is well reproduced by the interferometer data. The maximum deviation to the reference value is 9%. The other averaged roughness parameters like rms roughness R_q which are not shown here have similar deviations. The average maximum height R_z and the maximum roughness depth R_{max} as peak values are up to 17% smaller than their reference values.

As shown above the use of the three-wavelength diode laser interferometer offers a measurement range of $\approx 145 \mu\text{m}$ and allows to measure objects not accessible to one-wavelength interferometers, i.e. surfaces with steps larger than half the optical wavelengths. Also, a temporary loss of signals, e.g. due to poor reflecting parts of the surface, only leads to missing data for these areas and does not interrupt the scan as it would be the case for a fringe counting method.

Although the interferometer itself has a resolution of about 4 nm and its expected uncertainty is of the order of 20 nm, the resulting overall accuracy is unfortunately limited by the mechanical translation stages used in the experiments to values up to 250 nm for scan lines longer than 4 mm.

The interferometer reaches its limits on rough surfaces. Such surfaces could be measured, although the interferometer signal amplitude fluctuated and dropped partially to 10% of the value on smooth areas. For a calculation of the roughness parameters fringe counting was applied to get equal spaced data without missing points. The roughness parameters derived from these values are in good agreement with the calibration values of the roughness standards.

4. PRECISE LENGTH MEASUREMENTS OF PRISMATIC BODIES

For many industrial applications precise measurement of prismatic bodies, e.g. gauge blocks, or cylindrical samples, by multi-wavelength interferometry is necessary for dissemination of the length unit metre, i.e. traceability of the length measurement. Precise length changes of such bodies with temperature (thermal expansion), pressure (compressibility), and time (long term stability) can be measured with PTB's Precision Interferometer. Fig.9 shows the interferometer situated in a temperature controlled and vacuum tight environmental chamber. The light provided by the three different lasers alternatively passes a fibre representing the entrance of the interferometer. The reference path of the interferometer can be varied for phase stepping by slightly tilting the compensation plate. The tilt angle is monitored by an auxiliary interferometer and servo controlled. For measurements in air the measuring path contains a 400 mm vacuum cell close to the sample to determine the refractive index of air in the specific environmental conditions.

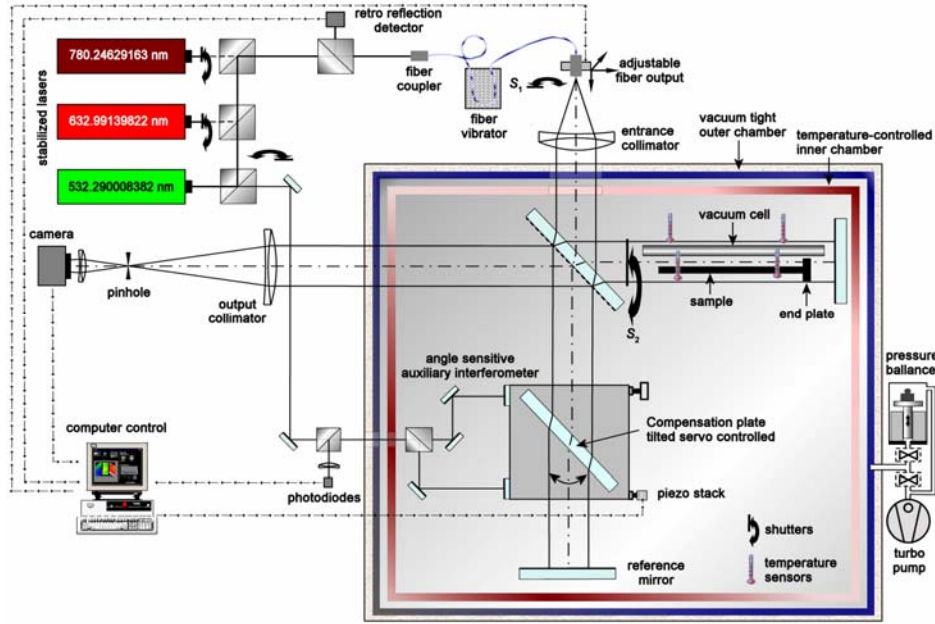


Fig.9 Scheme of PTB's Precision Interferometer

A 512 x 512 pixel camera system (Photometrics CH 350) provides data frames at 16-bit per pixel. Phase stepping interferometry based on intensity frames at 8 different phase steps is used to obtain the phase map of the sample including the end plate [12]. The centre position of the samples' front faces with respect to the camera pixel coordinates is assigned [13]. Interferometer autocollimation was adjusted by retroreflection scanning before a measurement was started [14].

Three stabilised lasers are used subsequently in the measurements. The gauge block lengths resulting from using the two J_2 -stabilised lasers at 532 nm and 633 nm were averaged. The Rb-stabilised laser at 780 nm is used for a coincidence check only.

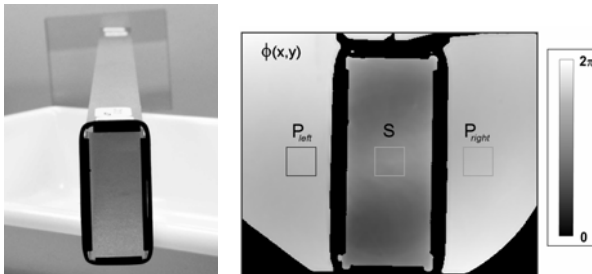


Fig.10 Left: front view of the sample wrung to the end plate, right: measured interferogram with a region of interest (ROI) at the sample's front face (S) and two symmetrically arranged ROIs at the end plate ($P_{\text{left/right}}$)

The fractional order of interference, f , can be extracted from the interferogram. Fig.10, left, shows a photograph of a typical sample. On the right-hand side of Fig.10 the measured interferogram of this sample is shown. The rectangles indicate the regions of interest (ROIs) in which the phase values are averaged. This leads to the values ϕ_S , ϕ_p^{left} , and ϕ_p^{right} from which the fractional order of interference is calculated:

$$f = \frac{1}{2\pi} \left[\frac{1}{2} (\phi_p^{\text{left}} + \phi_p^{\text{right}}) - \phi_S \right] \quad (9)$$

Using optical interferometry, the length L of a sample body is expressed as a multiple of the light wavelength used. For one-wavelength interferometry the exact knowledge of the integer interference order (entailed with a precision mechanical pre-measurement) would be required before the exact length can be determined according to (1). The use of different wavelengths, however, results in independent lengths $L_k = \frac{1}{2} \lambda_k (i_k + f_k)$ which should coincide. The expected coincidence is predicted by the uncertainties for the individual λ_k and f_k , respectively. A variation technique can be used for the extraction of the integer orders of interference known as "method of exact fractions". Here, integer variation numbers δ_k are introduced in the length evaluation:

$$L_k = \frac{1}{2} \lambda_k (i_k + \delta_k + f_k) \quad (10)$$

in which i_k is evaluated from the estimated length

$i_k = L^{\text{est}} / \frac{1}{2} \lambda_k$. At a set of $\{\delta_1, \delta_2, \dots\}$ the mean length is calculated:

$$\bar{L} = \frac{1}{r} \sum_{k=1}^r L_k \quad (11)$$

and the average deviation of L_k from \bar{L} can be used as a coincidence value:

$$\Delta = \frac{1}{r} \sum_{k=1}^r |\bar{L} - L_k| \quad (12)$$

Fig.11 shows a measurement example in which two wavelengths ($r = 2$) are used as a light source subsequently. The estimate of the sample body's length is 299.15 mm. The measured fractional orders are given in Table 2 for $k = 1$ and $k = 2$.

Fig.11 reveals periodic coincidence values near zero which are separated by about 12 μm from each other. It is noticed that, before these minima are identified with possible lengths, it is necessary to review the length uncertainty caused fractional orders of interference. From (1) follows:

$$u(L_k)^2 = (L^{\text{est}} u(\lambda_k) / \lambda_k)^2 + \left(\frac{1}{2} \lambda_k u(f_k) \right)^2 \quad (13)$$

and, in case of the mentioned example, the uncertainties $u(L_k)$ are close to 0.1 nm as depicted in the last column in Table 2.

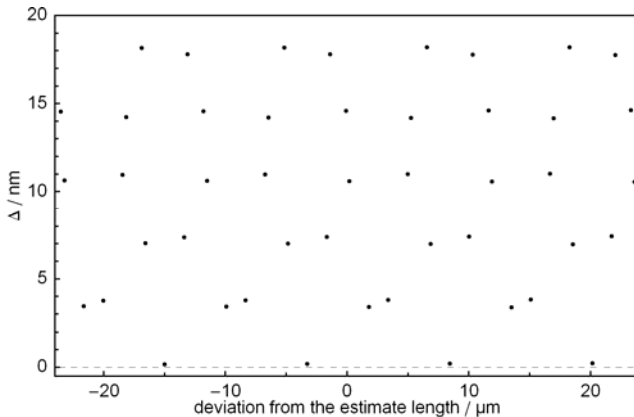


Fig.11 The average length resulting from variations of the integer orders (x-coordinates of the data points) and the related average deviation (y-coordinates of the data points) when two different wavelength are applied.

Accordingly, the periodic minima separated by about 12 μm in Fig.11 actually represent possible alternatives for the length of the sample body.

TABLE 2
k λ_k / nm $u(\lambda_k) / \lambda_k$ f_k $u(f_k)$ $u(L_k) / \text{nm}$
(in example) m
(in example)

k	λ_k / nm	$u(\lambda_k) / \lambda_k$	f_k	$u(f_k)$	$u(L_k) / \text{nm}$	m (in example)
1	532.290008382	3e-12	0.0271	0.0003	0.08	
2	632.99139822	2.5e-11	0.1723	0.0004	0.13	
3	780.24629163	1e-9	0.6465	0.0006	0.38	

Such a range of unambiguity, i.e. 12 μm , is not only much larger than one order of interference ($\approx 0.3 \mu\text{m}$), it is also clearly larger than the half-synthetic wavelength of the same two wavelengths which is about 1.7 μm . In order to elaborate the difference between such coincidence interval and the half of the synthetic wavelength, Fig.12 shows the course of the periodic interference intensities (solid curves) together with the respective interference phase modulo 2π (grey scales) for the same two wavelengths as used for the method of exact fractions in Fig.11 (from Table 1 for $k = 1$ and $k = 2$). Accordingly, it becomes clear that the synthetic wavelength, indicated λ_{synth} in Fig.12, represents the period defined by the condition that the fractional orders of interference coincide (same greylevel at positions $k \times \lambda_{\text{synth}} / 2$). This kind of "phase coincidence" is basically different from the coincidence of lengths used as criteria in the method of exact fractions via (1). On the other hand the coincidence interval of about 12 μm visible in Fig.11 is a multiple of the half synthetic wavelength. It can be looked upon the recovery period of both interference phases to the same values as visible in Fig.12 for $0 \times \lambda_{\text{synth}} / 2$

and $7 \times \lambda_{\text{synth}} / 2$. However, the actual number of k in $k \times \lambda_{\text{synth}} / 2$ again depends on the sharpness of a "phase coincidence recovery criterion". Such criterion in principle means the same as the criterion for length coincidence via (12).

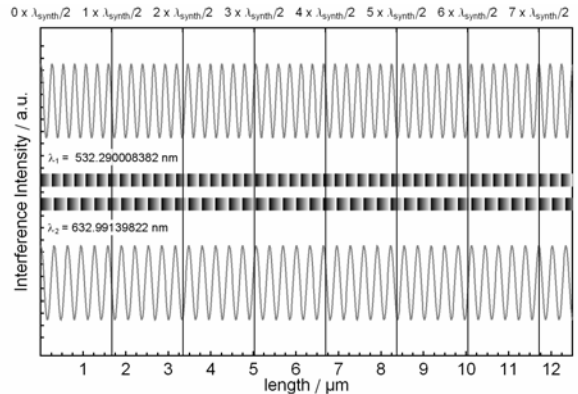


Fig.12 The average length resulting from variations of the integer orders (x-coordinates of the data points) and the related average deviation.

The range of unambiguity is further enlarged when a third wavelength is used in addition. Applying the same length coincidence criteria as for the two wavelength above (see Fig.11) the three wavelength method leads to the data points depicted in Fig.13.

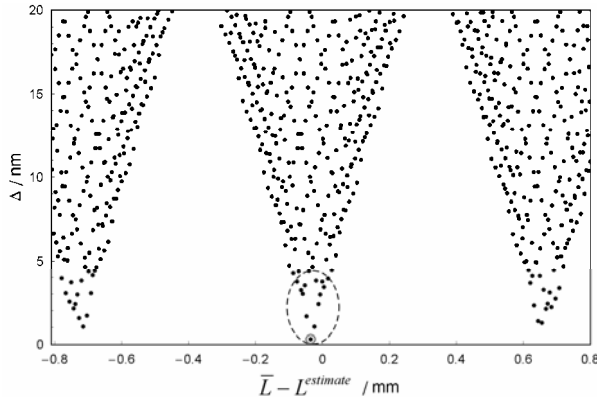


Fig.13 The average length resulting from variations of the integer orders (x-coordinates of the data points) and the related average deviation.

Again, a large number of values exist below a level Δ of 5 nm (data points within the dashed ellipse in Fig.13). The x-values of these points are separated by some tens of micrometer. However, certain minima of Δ exist, the separation of which exceeding very large values of more than 0.6 mm. It is again tempting to identify the minimum closest to L^{est} with the length of the sample. However, such conclusion requires very low uncertainties of $u(L_k)$ as can be achieved with the Precision Interferometer as depicted in Table 2. The actual minimum, Δ_{min} , is about 0.3 nm (see the data point marked by the grey circle in Fig.13). This value is somewhat larger than the total uncertainty of the mean length resulting to:

$$u(\bar{L}) = \frac{1}{3} \sqrt{\sum_{k=1}^3 u(L_k)^2} \approx 0.14 \text{ nm} \quad (14)$$

The reason for this somewhat larger value of Δ_{min} compared to 0.14 nm can be attributed to small constant influences onto the coincidence between the different lengths L_k as discussed in [15].

The low value of $u(\bar{L})$ together with the fact that the neighbouring points are off by more than 1 nm (see data points within the dashed circle of Fig.13) justifies the conclusion that the mean length for which Δ_{min} is found can be looked upon the actual length. Thus, the range of unambiguity is in fact about 0.6 mm as assumed in the above example. Therefore, a rough estimate of the length, obtained from a simple measurement, is sufficient for measurements at PTB's Precision Interferometer.

5. CONCLUSIONS

The multi-wavelength measurement technique is a proper method to remove ambiguity in interferometric length measurements. In general, the more accurate the fractions of the fringes can be measured, the larger is the range of unambiguity.

An absolute distance interferometer has been developed for the measurement of long distances of up to approx. 10 m by combination of frequency-sweeping interferometry and two-wavelength interferometry, using two external cavity diode lasers emitting at 776 nm and 770 nm. A comparison of the absolute distance interferometer to a counting HeNe laser interferometer shows a deviation below 0.5 μm + 0.5 $\mu\text{m}/\text{m}$ up to 10 m.

A three-wavelength diode laser interferometer has been developed for the measurement of surface profiles using parameter stabilised diode lasers (789.5 nm, 822.95 nm, and 825.3 nm). An uncertainty of approx. 20 nm was achieved for a measuring range below 150 μm . This "diode laser profilometer" was tested using a PTB depth setting standard. The reference values of the standard agree well within its uncertainty with the values of the profilometer. Surface measurements on a PTB superfine roughness standard show that the diode laser profilometer reaches its limits on rough surfaces with an average maximum height R_z above 450 nm.

Using PTB's Precision Interferometer for measurements of the length of bodies with parallel end faces (prismatic bodies) the measurement uncertainty of the averaged length is quite below 0.3 nm. Accordingly, the range of unambiguity is enlarged depending on the number of wavelengths applied. It is demonstrated that for two wavelengths, i.e. 532 nm and 633 nm, the range of unambiguity resulting from the method of exact fraction is a multiple of the synthetic wavelength. When three wavelengths, i.e. 532 nm, 633 nm, and 780 nm, are used the range of unambiguity enlarges drastically to more than 0.5 mm. Therefore, for ultra precise length measurements at PTB's Precision Interferometer a rough estimate of the length is sufficient.

ACKNOWLEDGEMENTS

The authors are grateful to the Deutsche Forschungsgemeinschaft (DFG) for financial support.

REFERENCES

- [1] Abou-Zeid, A. (1988). Diode lasers for interferometry. *J. of Precision Engineering*, 11 (3), 139.
- [2] Bodermann, B., Burgarth, V., Abou-Zeid, A. (2001). Modulation-free stabilised diode laser for interferometry using Doppler-reduced Rb transitions. In Balsamo, A. et al (eds.) *Proc. 2nd Euspen Topical Conference*. Turin, Italy, Vol. 1, 294–297.

- [3] Zarka, A., Abou-Zeid, A. et al (2000). International comparison of eight semiconductor lasers stabilised on 12712 at 633 nm. *Metrologia*, 37 (4), 329.
- [4] Bourdet, G.L., Orszag, A.G. (1979). Absolute distance measurements by CO₂ laser multiwavelength interferometry. *Applied Optics* 18, 225–227.
- [5] Bechstein, K.H., Fuchs, W. (1998). Absolute interferometric distance measurements applying a variable synthetic wavelength. *Journal of Optics* 29, 179–182.
- [6] Kinder, T., Salewski, K.D. (2002). Absolute distance interferometer with grating stabilised tunable diode laser at 633 nm. *Journal of Optics A: Pure and Applied Optics* 4, 364–368.
- [7] Hartmann, L., Meiners-Hagen, K., Abou-Zeid, A. (2008). An absolute distance interferometer with two external cavity diode lasers. *Measurement Science and Technology* 19, 045307.
- [8] Bönsch, G., Potulski, E. (1998). Measurement of the refractive index of air and comparison with modified Edlens formulae. *Metrologia* 35, 133–139.
- [9] Heydemann, P.L.M. (1981). Determination and correction of quadrature fringe measurement errors in interferometers. *Applied Optics* 20, 3382–3384.
- [10] Meiners-Hagen, K., Burgarth, V., Abou-Zeid, A. (2004). Profilometry with a multi-wavelength diode laser interferometer. *Measurement Science and Technology* 15, 741–746.
- [11] Abou-Zeid, A., Wolf, M. (2004). Profilometry: using a diode laser interferometer with three wavelengths. In De Chiffre, L., Carneiro, K. (eds.) *Proc. 1st Euspen Topical Conference on Fabrication and Metrology in Nanotechnology*. Copenhagen, Denmark, Vol. 1, 137–140.
- [12] Schödel, R., Nicolaus, A., Bönsch, G. (2002). Phase stepping interferometry: Methods to reduce errors caused by camera nonlinearities. *Applied Optics* 41, 55–63.
- [13] Schödel, R., Decker, J.E. (2004). Methods to recognize the sample position for most precise interferometric length measurements. In *Proceedings of SPIE*. Vol. 5532, 237–247.
- [14] Schödel, R., Bönsch, G. (2004). Highest accuracy interferometer alignment by retroreflection scanning. *Applied Optics* 43, 5738–5743.
- [15] Schödel, R., Nicolaus, A., Bönsch, G. (2003). Minimizing interferometer misalignment errors for measurement of sub-nanometer length changes. In *Proceedings of SPIE*. Vol. 5190, 34–42.